DOI: 10.1002/chem.201002151

Kinetics from Indirectly Detected Hyperpolarized NMR Spectroscopy by Using Spatially Selective Coherence Transfers

Talia Harris,[a] Patrick Giraudeau,[a, b] and Lucio Frydman*[a]

Abstract: An important recent development in NMR spectroscopy is the advent of ex situ dynamic nuclear polarization (DNP) approaches, which are capable of yielding liquid-state sensitivities that exceed considerably those afforded by the highest-field spectrometers. This increase in sensitivity has triggered new research avenues, particularly concerning the in vivo monitoring of metabolism and disease by NMR spectroscopy. So far such gains have mainly materialized for experiments that focus on nonprotonated, low-γ nuclei; targets favored by relatively long relaxation times T_1, which enable them to withstand the transfer from the cryogenic hyperpolarizer to the reacting centers of interest. Recent studies have also shown that transferring this hyperpolarization to protons by indirectly detected methods could successfully give rise to ^{1}H NMR spectra of hyperpolarized compounds with a high sensitivity. The present study demonstrates that, when merged with spatially encoded methods, indirectly detected ^{1}H NMR spectroscopy can also be exploited as time-resolved hyperpolarized spectroscopy. A methodology is thus introduced that can successfully deliver a series of hyperpolarized ^{1}H NMR spectra over a minutes-long timescale. The principles and opportunities presented by this approach are exemplified by following the in vitro phosphorylation of choline by choline kinase, a potential metabolic marker of cancer; and by tracking acetylcholine's hydrolysis by acetylcholine esterase, an important enzyme partaking in synaptic transmission and neuronal degradation.

Keywords: dynamic nuclear polarization · enzyme catalysis · NMR spectroscopy · spatial encoding · time-resolved spectroscopy

Introduction

Continuous efforts are being invested towards developing new approaches with improved abilities to characterize dynamic biochemical processes in general, and in vivo metabolism in particular. These tools can find use in biological research, as well as in clinical applications that assess disease and its response to therapeutic treatments. For several decades, NMR spectroscopy and magnetic resonance imaging (MRI) have served as central methods to enable such studies; both in vitro, as well as in animal and human metabolic settings.[1,2] The atomic site specificities carried by NMR's chemical shifts, coupled with the spatial localization capabilities that arise upon the employment of magnetic field gradients, have been key ingredients in enabling these applications. Further progress in this usage of NMR spectroscopy and of MRI hinges on improving the information available from these techniques. Particularly pressing is the need to enhance the sensitivity of NMR spectroscopy, given the weak signals associated with these experiments and the low natural concentrations of typical metabolic markers. Recent years have witnessed what promises to become a major thrust of these efforts, with emerging alternatives capable of preparing nuclei in "hyperpolarized" liquid-phase states. These are metastable spin arrangements in which the bulk nuclear polarizations depart from their usual (ca. 10^{-5}) Boltzmann distributions, and approach unity values.[3] Once prepared and transferred into an NMR/MRI scanner, the "super-signals" that can be elicited from these spin arrangements can be exploited within a timescale dependent on the longitudinal relaxation time T_1 of the hyperpolarized nuclei. Methods proposed and demonstrated for producing and exploiting these extreme spin-polarization levels under in vivo compatible conditions include the use of parahydrogen,[4,5]

[a] T. Harris, Dr. P. Giraudeau, Prof. L. Frydman
Department of Chemical Physics
Weizmann Institute
Rehovot, 76100 (ISRAEL)
Fax: (+972)-8-934-4123
E-mail: lucio.frydman@weizmann.ac.il

[b] Dr. P. Giraudeau
CEISAM
UMR CNRS 6230
University of Nantes (France)

the optical pumping of noble gases,[6,7] and microwave-driven dynamic nuclear polarization (DNP) from unpaired electrons.[8–10] Of these methods, the last option has the appeal of providing high enhancements while making few demands in terms of chemical substrate or sample preparation. Several in situ or ex situ experimental approaches have been proposed to perform DNP prior to NMR spectroscopic acquisition.[11] Particularly promising have been the metabolic results afforded by the ex situ DNP approach proposed by Golman et al.,[12] whereby the sample to be analyzed is comixed with a free radical, frozen in a glass at cryogenic temperatures, and hyperpolarized by irradiating the radical close to its unpaired electron's Larmor frequency for relatively long periods of time. Rapid melting and shuttling of the nuclear spins from this cryogenic environment into a scanner enables an otherwise routine solution-state NMR spectroscopic or MRI observation.[12,13] Yet, upon taking into account the effects of the cryogenic cooling and of the DNP process, these "routine" observations will take place on nuclei the polarization of which has been enhanced by a factor of around $(\gamma_{electron}/\gamma_{nucleus}) \times (B_{DNP}T_{NMR}/B_{NMR}T_{DNP})$, or the equivalent of around $10^4\times$ magnification.

Despite its outstanding promise, the time needed for ex situ DNP to transfer the sample from the polarizer to the NMR/MRI scanner, combined with the delays that may be subsequently needed for monitoring the ensuing metabolic processes, implies that only sites with relatively long liquid-state T_1s will be capable of retaining a significant hyperpolarization. For this reason, hyperpolarized metabolic studies have focused principally on nonprotonated low-γ nuclei, such as the ^{13}C of carbonyls or the ^{15}N of quaternary amines.[14–27] While bearing an exciting potential for improving high-resolution liquid-state NMR spectroscopy sensitivity in general, and in vivo spectroscopy in particular, these procedures appear to leave aside the important realm of ^1H NMR spectroscopy. This is a considerable drawback given that this spectroscopy 1) is associated with the highest-sensitivity target in all NMR spectroscopy, 2) utilizes the most common hardware available in MRI scanners, and 3) may be characterized by better spectral and much superior spatial resolutions than those associated with measurements on low-γ counterparts. The first of these features, in particular, has made so-called inverse methods of detections (whereby NMR information initially encoded on low-γ nuclei is transferred to ^1H nuclei for final detection) a mainstream approach in analytical and biomolecular studies.[28–30] This promising alternative has also been recently explored within the contexts of DNP- and para-hydrogen-enhanced hyperpolarized NMR spectroscopy,[31,32] in which advantages could result from storing the hyperpolarization in low-γ nuclei capable of undergoing an efficient enhancement, and retaining it for the long timescale compatible with metabolic processes, and then transferring it to nearby protons on which the NMR measurements are actually made.[33] Herein, we further explore the usefulness of these approaches, particularly in combination with new methods capable of repeatedly transferring aliquots of the low-γ spin hyperpolarization to neighboring protons by using spatially selective principles. This maximizes the efficiency of the transfer while providing the temporal dimension needed for carrying out metabolic characterizations. The potential offered by these new spectroscopic approaches is illustrated by hyperpolarized NMR spectroscopy measurements of two choline-related enzymatic reactions involved in cancer metabolism and in neuronal transmission.

Results and Discussion

Scheme 1 illustrates the kind of problems this study attempts to tackle and the methods adopted to address them. These are all water-soluble metabolites with a number of distinct biological roles: choline plays an integral part in methyl-transfer metabolism; its transformation to phosphocholine is an essential step in the formation of lipids making up cell membranes,[34] and in its acetylated form it is a principal brain neurotransmitter.[35] Moreover, an aberrant metabolism of choline is associated with a number of illnesses: the choline↔phosphocholine transformation has been shown to be upregulated in cancerous cells,[36,37] and alterations in the choline↔acetylcholine interconversion have been found in Alzheimer's and Parkinson's diseases.[38,39] When viewed as a potential target for ex situ DNP hyperpolarization, choline shows great promise: it possesses a non-protonated nitrogen that has been shown to undergo efficient hyperpolarization, and is endowed with very long T_1 relaxation times ranging from about 150 s in the molecules' protonated forms to around twice this time upon perdeuteration.[19] Figure 1 gives an idea of the sensitivity enhancements and long probing times that can be necessary for this site, for the Hypersense and 11.7 T Varian DNP NMR setup used in this study. The interest of detecting this polarization enhancement for in vivo studies has been very recently highlighted.[40]

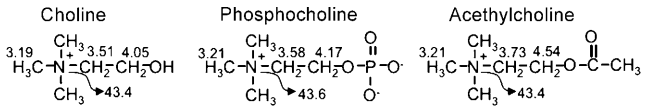

Scheme 1. Choline derivatives analyzed in this study, and the ^1H and ^{15}N NMR chemical shifts associated with each structure.

In spite of this potential, choline's ^{15}N site is ill-positioned for following the acetylation or phosphorylation reactions that one might be interested to quantify in metabolic settings. Both of these processes take place on the molecule's hydroxyl site, and result in the minor ^{15}N NMR shift effects summarized in Scheme 1. In contrast, much larger shift changes affect the protons bonded to the C2 sites of these molecules, because they are closer to the hydroxyl epicenter of the metabolic transformations. This chemical-shift data highlights the convenience of exploiting choline's slowly re-

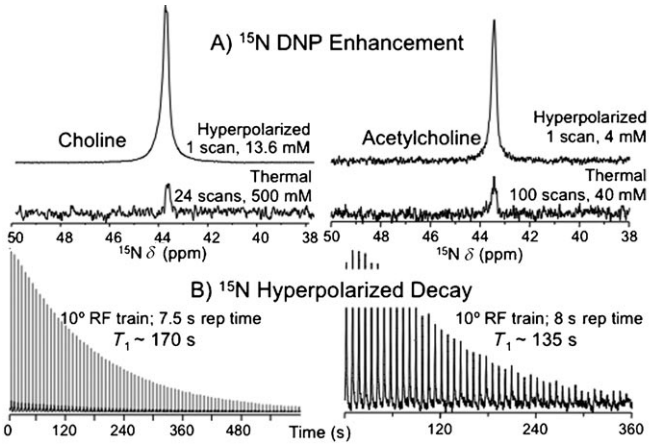

Figure 1. A) Comparison between conventional (bottom) and hyperpolarized (top) ^{15}N NMR spectra arising from choline and acetylcholine for the indicated concentrations and number of signal averages. On the basis of the signal to noise ratios measured in each trace, polarization enhancement factors of 5500× and 6000× could be inferred for each of these compounds. B) T_1-driven decay of the ^{15}N hyperpolarization of choline and acetylcholine, as measured by a train of single-pulse 1D NMR spectroscopy experiments applied after sample injection. Hyperpolarization arose from cofreezing the analytes with tris{8-carboxyl-2,2,6,6-tetra[2-(1-hydroxyethyl)]benzo(1,2-d:4,5-d′)bis(1,3)dithiole-4-yl}methyl sodium salt (trityl) in a 1:1 solution of D_2O/[D_6]DMSO, followed by irradiation for about 3 h at 94.188 GHz with 100 mW microwave power, and quickly dissolving them in either D_2O (left) or H_2O/tris(hydroxymethyl)aminomethane (tris) buffer (right) to the indicated final concentrations.

laxing hyperpolarized ^{15}N site as a source of enhanced NMR signal, while following the actual reaction process in an indirect detection mode that exploits the larger chemical-shift changes that the oxygen-bonded methylene protons will undergo upon reacting. As recently discussed elsewhere,[32,33] such information can be transferred through the small but non-negligible ^3J(N,H) couplings between the ^{15}N and the C2-bearing protons, by using either single-quantum INEPT-based or multiple-quantum DEPT-like processes. We chose to rely on the former, by exploring a spectrally selective version of the classical Freeman–Morris three ($\pi/2$) sequence [Eq. (1)]:[41]

$$\mathrm{N}_z(\mathrm{hyp}) \xrightarrow{(\pi/2)_x^{\mathrm{N}}} \mathrm{N}_y \xrightarrow{0.25/J,(\pi)^{\mathrm{N}}/(\pi)^{\mathrm{H}}_{\mathrm{sel}},0.25/J} 2\,\mathrm{H}_z\mathrm{N}_x \xrightarrow{(\pi/2)_y^{\mathrm{N}}(\pi/2)^{\mathrm{H}}} 2\mathrm{H}_x\mathrm{N}_z - \mathrm{Acq}(^1\mathrm{H}) \quad (1)$$

in which superscript indices denote the targeted species, subscript indices are relevant pulse phases, and 3 Hz is the approximate coupling measured between the ^{15}N and the pertinent ^{1}Hs. The sequence in Equation (1) begins from the hyperpolarized ^{15}N state, and relies on a selective ^{1}H π pulse applied on-resonance with the targeted methylenes for improving a transfer which, if broadband, would share a substantial part of the ^{15}N hyperpolarization with the more numerous (but otherwise uninformative) methyl protons. The heteronuclear transfer process in Equation (1) also provides an opportunity to use gradient-based coherence selection pulses for reducing the intense ^{1}H water peak and other background metabolite signals that could potentially obscure the relevant peaks. Figure 2 A illustrates the results of applying this sequence to hyperpolarized choline in D_2O and to acetylcholine dissolved in a buffered H_2O solution. Relative to conventional ^{1}H NMR spectra of the same sample, this sequence gives rise to a site-specific polarization enhancement of about 300. Although high, this enhancement still amounts to only around 50% of the maximum theoretical enhancement that one could expect from a full ^{15}N→^{1}H transfer. At the same time, however, the DNP-enhanced ^{1}H spectrum reveals an almost complete elimination of background signals, including the strong water peak that

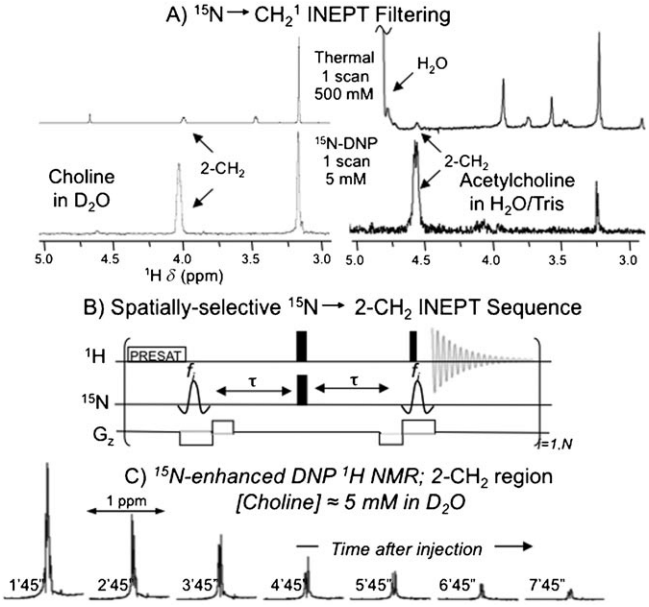

Figure 2. A) ^{1}H NMR spectra of choline and acetylcholine recorded at thermal equilibrium (top), and counterparts arising from an INEPT sequence [see Eq. (1)], starting from hyperpolarized ^{15}N, and using an optimized transfer of the spin order to the C2 methylene protons. Minor differences in the chemical shifts of the two spectra might reflect small differences in the samples' temperatures. B) The pulse sequence employed to transform the single-shot transfer used in A) into an experiment that makes multiple transfers of the ^{15}N hyperpolarization to these protons at various times: replacing the hard $(\pi/2)_N$ pulses of Equation (1) by selective ones applied at shifted frequencies $\{f\}_{i=1,N}$ in the presence of suitable field gradients opens the possibility of "drawing" magnetization from different sample positions over the long timescales supported by the ^{15}N T_1. Additional sequence components include a hard $(\pi)_N$ pulse that leaves the ^{15}N magnetization of all nonaddressed slices along $\pm z$, spectrally selective $(\pi)_H$ ^{1}H pulses that solely address the targeted methylene resonances (solid lines), a reliance on gradients that further purify the desired coherence transfer pathway, and a delay ($\tau = 32$ ms) optimized to transfer the hyperpolarization to the methylene protons. Immediate repetition of the sequence yielded a reference background, from which residual water signals were subtracted when necessary. C) Results obtained upon looping the pulse sequence in B) to extract ^{15}N-choline hyperpolarization at seven different times over lapses that exceed those supported by the natural T_1s of the targeted protons by orders of magnitude. The illustrated trace arose from applying 0.71 ms selective $(\pi/2)_N$ sinc pulses on a 5 mM hyperpolarized sample dissolved in D_2O; each of these was spaced by approximately 3 kHz frequency increments and applied in the presence of 35 G/cm gradients. The effective decay constant of the resulting data is $T_1^* = 125$ s.

resonates in the neighborhood of acetylcholine's diagnostic methylene 2-CH_2 peak.

This promise notwithstanding, the methylene enhancement observed in Figure 2A is ill-suited for acquiring the multiple scans that are needed for extracting metabolic information from hyperpolarized molecules. Indeed, for simple experiments, this can be accomplished by monitoring 1D spectra after applying a series of low-excitation-angle pulses on the hyperpolarized state. The sequence in Equation (1), on the other hand, relies on the use of two $(\pi/2)_N$ pulses and an optimized interpulse delay, which is meant to transfer the full polarization from the low-γ nucleus to the targeted ^{1}H nucleus. All the ex situ hyperpolarization is thus expended in a single shot. Options that could help in conserving the ^{15}N hyperpolarization, and that are compatible with indirect detection conditions, include reducing the pulse angles involved in the nuclear excitation, or choosing an interpulse delay that does not fully transfer the single-spin $^{15}N_z$ hyperpolarization into the single-quantum antiphase states involved in the subsequent ^{1}H detection. Both of these approaches, however, entail signal losses: reliance on ^{15}N pulses that are not $\pi/2$ rotations will dissipate portions of the low-γ hyperpolarization in a process that rapidly accumulates; keeping the use of the two $(\pi/2)_N$ pulses but manipulating their interpulse delay will transfer aliquots of magnetization, but will create, in the process, longitudinal $2N_zH_z$-like spin-order states, the decay of which will be dominated by the proton's T_1 and therefore be incompatible with the reaction timescales normally addressed by metabolism.

To bypass these constraints, we explored the integration of the DNP-enhanced indirect detection sequence sketched in Equation (1) with spatial-encoding techniques. Spatial encoding is an approach typically used to replace the serial incrementation of a temporal variable (for instance, the t_1 indirect domain typically changed by constant steps within 2D NMR sequences) with a spin coordinate position within the sample.[42,43] This can be implemented with the aid of imaging-like magnetic field gradients acting in combination with frequency-swept (or stepped) manipulations of the spins. Besides enabling the recording of arbitrary multidimensional NMR spectra within a single scan (including the indirectly detected acquisition of 2D NMR correlations on DNP-hyperpolarized samples[44–46]), spatially encoded methods can deliver in a single shot an array of inversion–recovery T_1 measurements, or multiple-exchange 2D NMR spectra as a function of their intervening mixing periods.[47–49] In a similar spirit to these latter studies, the sequence in Figure 2B explores the opportunities that spatially selective manipulations open for measuring a kinetic series, starting from a singly hyperpolarized injected sample. This experiment involves a simple modification of the sequence in Equation (1), whereby the two $(\pi/2)_N$ manipulations have been made spatially selective. The main consequence of introducing this modification is to enable the acquisition of a series of experiments like the one illustrated in Figure 2A, each of these arising from a different location within the targeted sample. This approach presents some similarities with the strategy recently proposed by Panek et al. to include slice selection in single-scan experiments on hyperpolarized samples.[50] Figure 2C shows ^{1}H NMR results obtained upon executing this sequence on a sample of hyperpolarized choline: as can be appreciated, a clean series of informative methylene ^{1}H NMR spectra with good sensitivity is observed; these are characterized by the long lifetimes supported by the extreme T_1 of the ^{15}N site acting as their source of hyperpolarization.

Note that there are characteristic losses that (beyond the T_1 decay) may arise with this kind of approach. Diffusion, in particular, is a potential source of loss that could affect experiments of this kind through two main mechanisms: one involves spatial displacements of the spins before the magnetization windings that derive from the application of gradients have been refocused; the other involves molecular displacements of the spins from their ideal positions to be targeted by the selective pulses to unintended regions that are not meant to be addressed. The first kind of phenomena, which are usually the main source of signal loss in gradient-based NMR spectroscopy measurements, are essentially absent in these experiments because of the immediate refocusing gradients applied in conjunction with the excitation/storage pulses that are used to select the spatial slices (Figure 2B). The second mechanism would become active if 1) spins are displaced in between the spatially selective ^{15}N excitation and storage pulses that address a given slice, or 2) or spins undergo considerable displacement between the consecutive slice-selective scans that follow the common hyperpolarization process. To estimate how much such displacement effects would influence the experiment's sensitivity, we consider a fast water-like diffusion coefficient ($D \approx 10^{-5}$ cm^{2}s^{-1}), and rely on Fick's Law, $N(z,t) = N(z,0)*[1-\mathrm{erf}(z/\sqrt{(4Dt)})]$, to evaluate particle dispersion for the relevant time- and length-scales, in which t was assumed to be around 0.05 s for the RF interpulse delay, 100 s for the interscan delay, and Δz around 2.25 mm for the slab thickness (which was the smallest value used throughout our experiments; larger slabs should be less affected by these kind of "edge effects"). Under these assumptions it follows that the interpulse diffusion effects will be $< 0.2\,\%$, which is fully negligible; the interscan effects in contrast are much larger and should result in signal losses of around 9% relative to the full, integrated ideal signal. These losses stem from the fact that, in the aforementioned interscan delay, a portion of the hyperpolarized sample will migrate away from the targeted slab, and be replaced with spins that arise from an expended slab entering with negligible polarization. Effects of such magnitude might be visible, and may be partly responsible for the slightly different effective T_1s that could be derived from small-angle measurements like those in Figure 1B (ca. 170 s) as opposed to those arising from the spatially selective measurements in Figure 2C (ca. 125 s). This difference, however, probably also reflects the presence of other nonidealities (including pulse shaping and π-inversion-related losses in the latter sequences). Moreover, even

if quantitatively measurable, these diffusion effects should not bring about any noticeable distortions in the kinetics derived from these hyperpolarized NMR measurements. Indeed, this information will arise from measuring ratios between metabolic reactants and products; assuming that the D coefficients for these molecules are similar, these ratios should be, for all practical purposes, independent of all the diffusion effects considered in this paragraph.

With these considerations as background, we set out to explore the usefulness of this approach for monitoring metabolic processes. The first reaction targeted was the phosphorylation of choline by choline kinase. This same reaction has been utilized with hyperpolarized ^{15}N NMR spectroscopy,[19] and presents a good opportunity to follow the kinetics through both direct detection of the low-γ nucleus using a small-pulse-angle train, as well as through the indirectly detected ^{1}H NMR sequence introduced in Figure 2. Figure 3 summarizes results obtained for this system, and shows the expected decrease in the initial choline peak and a concomitant increase in the phosphocholine peak. This behavior is evidenced by both the ^{15}N direct-excitation hyperpolarized experiments, the spectra of which show the reactant and product peaks separated by 0.2 ppm (ca. 10 Hz at 11.7 T); as well as by the hyperpolarized ^{1}H methylene spectra, which show peaks separated by 0.12 ppm (60 Hz at 11.7 T). Good agreement can be seen between the kinetic results obtained by these directly and indirectly detected set of spectra, based on an integration of the resolved ^{1}H and ^{15}N resonances (see the data points in Figure 3C).

A second reaction that we targeted involved monitoring the hydrolysis of acetylcholine by an esterase. As the ^{15}N peaks of acetylcholine and choline are, in this instance, separated by $\leq$0.05 ppm (2.5 Hz at 11.7 T), it would be difficult or impossible to resolve these two species by direct ^{15}N detection. In contrast, transferring the hyperpolarization to the methylene protons adjacent to the reacting hydroxyl group—separated in the two compounds by over 0.4 ppm—opens a new route to following these reaction kinetics. Crucial in this endeavor is the feasibility of probing the reaction in the presence of an efficient gradient-driven suppression of the water resonance, which falls less than 0.25 ppm away from the product peak. The outcome of four consecutive reaction time points is illustrated in Figure 4B. Although direct comparison with the ^{15}N NMR results is not possible, there is good agreement between this data and longer-term ($\geq$300 s) observations based on the direct ^{1}H NMR detection of the reaction products.

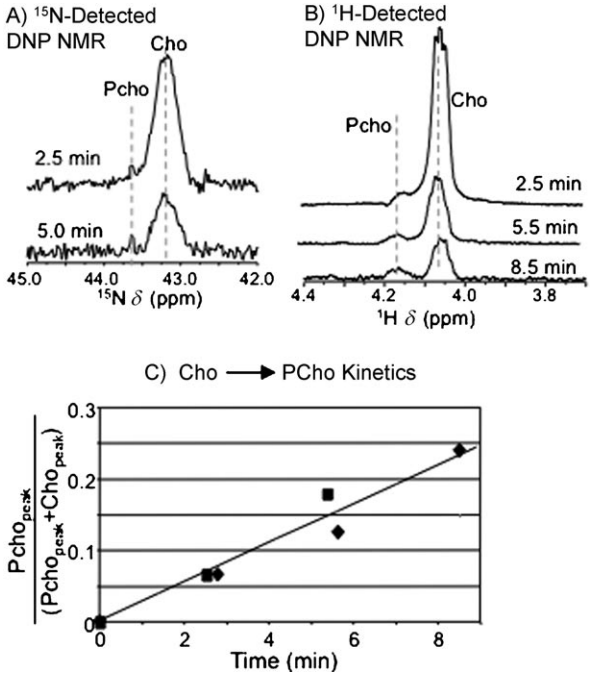

Figure 3. NMR spectral changes revealed by a 5 mM solution of hyperpolarized choline upon undergoing phosphorylation by 0.5 units of choline kinase. A) Emergence of the new phosphocholine resonance shown by directly detected single-pulse ^{15}N NMR spectroscopy experiments. B) Emergence of the ^{1}H NMR resonance associated with the methylenes in the C2-position of phosphocholine, as revealed by the indirect detection sequence introduced in Figure 2B. C) Comparison between the expected enzyme kinetics of kinase with results afforded by the ^{15}N- (■) and ^{1}H-detected (◆) hyperpolarized experiments, as derived from the relative peak ratios of the NMR peaks in A) and B). The straight line illustrates the best fit of the combined set of data points, and corresponds to an initial phosphorylation rate of 0.3 μmol min^{-1} under these conditions.

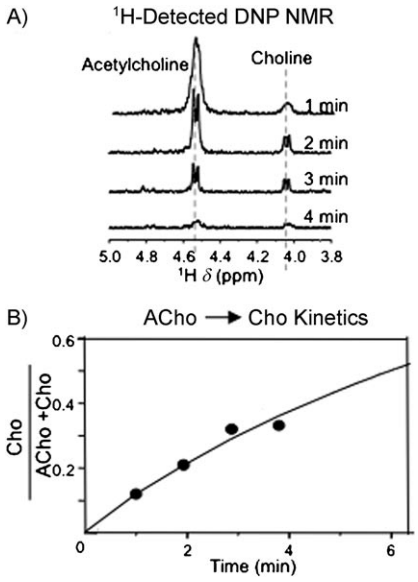

Figure 4. A) Spectral changes seen for hyperpolarized acetylcholine upon undergoing deacetylation into choline, under the action of 0.6 units of acetylcholine esterase. The ^{15}N-enhanced ^{1}H spectra only show resonances associated with the methylenes in the C2 position, as revealed by the indirect detection sequence introduced in Figure 2B. B) Comparison between the enzymatic kinetic results afforded by the indirectly detected hyperpolarized experiments in A), and the enzymatic activity rate observed by conventional ^{1}H NMR (●) spectroscopy at longer reaction/signal-averaging times ($\geq$200 s). Under the assayed conditions, these data (straight line) indicate a deacetylation rate of 0.12 μmol min^{-1}.

Conclusion

The data summarized in Figures 2–4 may open up valuable new opportunities in the field of metabolic NMR spectroscopy, since they show that the unique sensitivity enhancement afforded by ex situ DNP can be combined with the long lifetimes typical of low-γ heteronuclei, as well as with the wealth of information and additional sensitivity that characterizes indirect detection. Neither the sequences nor the principles involved in these new experiments are particularly complex, but the resulting data is unique. Although exemplified for the case of a quaternary ^{15}N site, similar advantages may also be brought to bear for other sites, including hyperpolarized carbonyl ^{13}C groups adjacent to methylene or methyl groups (e.g., acetates) or ^{15}N sites in aromatic bases.

A particularly encouraging feature of our approach is that, by transferring the observation of the signal to ^{1}H nuclei, these experiments become compatible with the receivers that are normally available in MRI scanners. This hardware, which has been highly optimized over the years, would still have to be complemented with low-γ irradiation facilities for performing the INEPT-derived sequences, but this can often be carried out in an ad hoc, less demanding fashion. Moreover, ^{1}H-based detection would enable optimal use of a scanner's field gradients, both for spatial localization as well as for suppression of background resonances through coherence-selective gradients. The spatial nature of the features exploited in this study has its own challenges, which include complications that may arise in vivo if the spatial homogeneity present in the in vitro setup analyzed in this work is absent. Still, a built-in way to compensate for such spatial heterogeneity effects arises from the reliance of this approach on measuring the ratio between the signal intensities of the reactant and product to extract its kinetic information. Assuming that these metabolites share similar diffusion and/or flow characteristics, this normalization would also account to a large extent for interpulse and even interscan molecular displacements. These hypotheses and further uses of the presented approach are currently being explored.

Experimental Section

Materials: This study focused on ^{15}N-labeled choline (Sigma Aldrich) and on ^{15}N-labeled acetylcholine. The latter was prepared by coevaporating ^{15}N-choline chloride with absolute ethanol and further drying under vacuum at 45 °C. The resulting salt (40 mg) was suspended in anhydrous Cl_2CH_2 (2 mL) under nitrogen, and acetylated with CH_3COCl (0.3 mL) overnight. To ensure full acetylation, this treatment was repeated twice. Solvents were then removed at reduced pressure and the residue was once again coevaporated with ethanol and dried under vacuum to yield ^{15}N-acetylcholine chloride as a white crystalline solid. Hyperpolarized samples of ^{15}N-labeled choline and acetylcholine were then studied on being subjected to enzymatic reactions by kinases and esterases, respectively. The choline kinase (Sigma) experiments were carried out in buffered solutions in H_2O (pH 8) that contained, once inside the NMR spectrometer, concentrations of 5 mM hyperpolarized choline, 100 mM tris, 100 mM KCl, 50 mM $MgCl_2$, and 10 mM ATP. For the esterase experiments, acetylcholine esterase (Sigma) was also prepared in a buffered aqueous solution (pH 7) to give, after hyperpolarization, final solution concentrations of 4 mM acetylcholine, 40 mM tris and 0.5 % Triton X-100.

Spectroscopic methods: DNP-enhanced NMR spectroscopy experiments were performed by using an OIMBL Hypersense polarizer operating at 1.5 K and a nominal electron Larmor frequency of 94 GHz. Hyperpolarization was implemented on 1.5 and 0.56 M solutions of ^{15}N-labeled choline and acetylcholine, respectively, which were prepared in a 1/1 D_2O/$[D_6]$DMSO solvent together with 20 mM of OX063 trityl radical.[51] Typical experiments utilized 5–20 μL aliquots of these solutions. Following DNP hyperpolarization the samples were transferred with 3 mL of pressurized water vapor (10 bar) into 5 mm NMR tubes, to give approximately 2 mL sample volumes (final concentrations indicated throughout the paper). A 500 MHz Varian Inova spectrometer equipped with an inverse HCN triple-resonance triple-axis gradient probe was employed in these NMR spectroscopy experiments. In a typical run, about 2.5 s would elapse between triggering the sample's melting/transfer process, and filling the NMR sample tube. Given the much longer timescales supported by the hyperpolarized ^{15}N T_1s, an additional delay of about 10 s would be usually taken for homogenizing the sample outside the NMR magnet, and another 30 s would be devoted to locking/shimming the spectrometer before starting the NMR pulse sequences. Various other parameters required for executing the experiments introduced in this work (radiofrequency offsets and shapes, gradient strengths, etc.) were calibrated prior to the injections using a reference 0.5 M ^{15}N-choline sample and standard procedures.

Acknowledgements

We are grateful to Prof. Hadassa Degani (Weizmann Institute, Biological Regulation) for the generous gift of choline kinase, to Dr. Veronica Frydman (Weizmann Institute, Research Infrastructures) for the preparation of the ^{15}N-labeled acetylcholine, and to Dr. Rachel Katz-Brull (Hebrew University - Hadassa Medical Center) and Prof. Geoffrey Bodenhausen (EPFL, Lausanne) for valuable discussions. This research was supported by the Israel Science Foundation (ISF 447/09), by a Helen and Martin Kimmel Award for Innovative Investigation, and by the generosity of the Perlman Family Foundation. P.G. acknowledges the Weizmann Feinberg Graduate School and the French Ministry of Foreign and European Affairs (Lavoisier program) for fellowships.

[1] R. A. de Graaf, *In Vivo NMR Spectroscopy: Principles and Techniques*, Wiley, New York, **1998**.
[2] R. G. Shulman, D. L. Rothman, *Metabolism by In Vivo NMR*, Wiley, New York, **2004**.
[3] W. Kockenberger, T. Prisner, *Appl. Magn. Reson.* **2008**, *34*, 213.
[4] C. R. Bowers, D. P. Weitekamp, *Phys. Rev. Lett.* **1986**, *57*, 2645.
[5] T. C. Eisenschmid, R. U. Kirss, P. P. Deutsch, S. I. Hommeltoft, R. Eisenberg, J. Bargon, R. G. Lawler, A. L. Balch, *J. Am. Chem. Soc.* **1987**, *109*, 8089.
[6] M. S. Albert, G. D. Cates, B. Driehuys, W. Happer, B. Saam, C. S. Springer, A. Wishnia, *Nature* **1994**, *370*, 199.
[7] G. Navon, Y.-Q. Song, T. Rõõm, S. Appelt, R. E. Taylor, A. Pines, *Science* **1996**, *271*.
[8] A. Abragam, M. Goldman, *Nuclear Magnetism: Order and Disorder*, Oxford University Press, Oxford, **1982**.
[9] T. R. Carver, C. P. Slichter, *Phys. Rev.* **1953**, *92*, 212.
[10] K. H. Hausser, D. Stehlik, *Adv. Magn. Reson.* **1968**, *3*, 79.
[11] R. G. Griffin, T. Prisner, *Phys. Chem. Chem. Phys.* **2010**, *12*, 5737.
[12] J. H. Ardenkjaer-Larsen, B. Fridlund, A. Gram, G. Hansson, L. Hansson, M. H. Lerche, R. Servin, M. Thaning, K. Golman, *Proc. Natl. Acad. Sci. USA* **2003**, *100*, 10158.
[13] J. Wolber, F. Ellner, B. Fridlund, A. Gram, H. Johannesson, G. Hansson, L. H. Hansson, M. H. Lerche, S. Mansson, R. Servin, M.

Thaning, K. Golman, J. H. Ardenkjaer-Larsen, *Nucl. Instr. and Meth. in Phys. A* **2004**, *526*, 173.
[14] M. J. Albers, R. Bok, A. P. Chen, C. H. Cunningham, M. L. Zierhut, V. Y. Zhang, S. J. Kohler, J. Tropp, R. E. Hurd, Y. F. Yen, *Cancer Res.* **2008**, *68*, 8607.
[15] P. Bhattacharya, E. Y. Chekmenev, W. H. Perman, K. C. Harris, A. P. Lin, V. A. Norton, C. T. Tan, B. D. Ross, D. P. Weitekamp, *J. Magn. Reson.* **2007**, *186*, 150.
[16] A. P. Chen, M. J. Albers, C. H. Cunnigham, S. J. Kohler, Y.-F. Yen, R. E. Hurd, J. Tropp, R. Bok, J. M. Pauly, S. J. Nelson, J. Kurhanewicz, D. B. Vigneron, *Magn. Reson. Med.* **2007**, *58*, 1099.
[17] A. P. Chen, J. Kurhanewicz, R. Bok, D. Xu, D. Joun, V. Zhang, S. J. Nelson, R. E. Hurd, D. B. Vigneron, *Magn. Reson. Imaging* **2008**, *26*, 721.
[18] S. E. Day, M. I. Kettunen, F. A. Gallagher, D.-E. Hu, M. Lerche, J. Wolber, K. Golman, J. H. Ardenkjaer-Larsen, K. M. Brindle, *Nat. Med.* **2007**, *13*, 1382.
[19] C. Gabellieri, S. Reynolds, A. Lavie, G. S. Payne, M. O. Leach, T. R. Eykyn, *J. Am. Chem. Soc.* **2008**, *130*, 4598.
[20] F. A. Gallagher, M. I. Kettunen, S. E. Day, M. Lerche, K. M. Brindle, *Magn. Reson. Med.* **2008**, *60*, 253.
[21] K. Golman, J. H. Ardenkjaer-Larsen, J. S. Petersson, S. Mansson, I. Leunbach, *Proc. Natl. Acad. Sci. USA* **2003**, *100*, 10435.
[22] K. Golman, J. S. Petersson, P. Magnusson, E. Johansson, P. Akeson, C. M. Chai, G. Hansson, S. Mansson, *Magn. Reson. Med.* **2008**, *59*, 1005.
[23] K. Golman, R. i. t. Zandt, M. Lerche, R. Pehrson, J. H. Ardenkjaer-Larsen, *Cancer Res.* **2006**, *66*, 10855.
[24] T. Harris, G. Eliyahu, L. Frydman, H. Degani, *Proc. Natl. Acad. Sci. USA* **2009**, *106*, 18131.
[25] S. J. Kohler, Y. Yen, J. Wolber, A. P. Chen, M. J. Albers, R. Bok, V. Zhang, J. Tropp, S. Nelson, D. B. Vigneron, *Magn. Reson. Med.* **2007**, *58*, 65.
[26] M. E. Merritt, C. Harrison, C. Storey, F. M. Jeffrey, A. D. Sherry, C. R. Malloy, *Proc. Natl. Acad. Sci. USA* **2007**, *104*, 19773.
[27] M. A. Schroeder, L. E. Cochlin, L. C. Heather, K. Clarke, G. K. Radda, D. J. Tyler, *Proc. Natl. Acad. Sci. USA* **2008**, *105*, 12051.
[28] G. Bodenhausen, D. J. Ruben, *Chem. Phys. Lett.* **1980**, *69*, 185.
[29] J. Cavanagh, W. J. Fairbrother, A. G. Palmer, N. J. Skelton, M. Rance, *Protein NMR spectroscopy: Principles and Practice*, Elsevier, Amsterdam, **2006**.
[30] L. Mueller, *J. Am. Chem. Soc.* **1979**, *101*, 4481.
[31] E. Y. Chekmenev, V. A. Norton, D. P. Weitekamp, P. Bhattacharya, *J. Am. Chem. Soc.* **2009**, *131*, 3164.
[32] R. Sarkar, A. Comment, P. R. Vasos, S. Jannin, R. Gruetter, G. Bodenhausen, H. Hall, D. Kirz, V. P. Denisov, *J. Am. Chem. Soc.* **2009**, *131*, 16014.
[33] J. A. Pfeilsticker, J. E. Ollerenshaw, V. A. Norton, D. P. Weitekamp, *J. Magn. Reson.* **2010**, *205*, 125.
[34] S. H. Zeisel, *Annu. Rev. Nutr.* **2006**, *26*, 229.
[35] M. Sarter, V. Parikh, *Nat. Rev. Neurosci.* **2005**, *6*, 48.
[36] G. Eliyahu, T. Kreizman, H. Degani, *Int. J. Cancer* **2007**, *120*, 1721.
[37] K. Glunde, M. A. Jacobs, Z. M. Bhujwalla, *Expert Rev. Molec. Diagnostics* **2006**, *6*, 821.
[38] K. Herholz, *Eur. J. Nucl. Med. Molec. Imag.* **2008**, 35, S25.
[39] H. Shimada, S. Hirano, H. Shinotoh, A. Aotsuka, K. Sato, N. Tanaka, T. Ota, M. Asahina, K. Fukushi, S. Kuwabara, *Neurology* **2009**, *73*, 273.
[40] C. Cudalbu, A. Comment, F. Kurdzesau, R. B. van Heeswijk, K. Uffman, S. Jannin, V. P. Denisov, D. Kirik, R. Gruetter, *Phys. Chem. Chem. Phys.* **2010**, *12*, 5818.
[41] G. A. Morris, R. Freeman, *J. Am. Chem. Soc.* **1979**, *101*, 760.
[42] L. Frydman, A. Lupulescu, T. Scherf, *J. Am. Chem. Soc.* **2003**, *125*, 9204.
[43] L. Frydman, T. Scherf, A. Lupulescu, *Proc. Natl. Acad. Sci. USA* **2002**, *99*, 15858.
[44] L. Frydman, D. Blazina, *Nat. Phys.* **2007**, *3*, 415.
[45] P. Giraudeau, Y. Shrot, L. Frydman, *J. Am. Chem. Soc.* **2009**, *131*, 13902.
[46] M. Mishkovsky, L. Frydman, *ChemPhysChem* **2008**, *9*, 2340.
[47] R. Bhattacharyya, A. Kumar, *Chem. Phys. Lett.* **2004**, *383*, 99.
[48] N. M. Loening, M. J. Thrippleton, J. Keeler, R. G. Griffin, *J. Magn. Reson.* **2003**, *164*, 321.
[49] B. Shapira, L. Frydman, *J. Magn. Reson.* **2003**, *165*, 320.
[50] R. Panek, J. Granwehr, J. Leggett, W. Kockenberger, *Phys. Chem. Chem. Phys.* **2010**, *12*, 5771.
[51] M. Thaning, U.S. Patent 6,013,810, **2000**.

Received: September 24, 2010
Published online: November 9, 2010

